Research Square

Preprints are preliminary reports that have not undergone peer review.
They should not be considered conclusive, used to inform clinical practice,
or referenced by the media as validated information.

Research on Optimization of Radial Uncoupled Charge Parameters Based on the Mechanical Characteristics of Step-Type Partitioning

Tao Wang

www.wthdbp@163.com

Wuhan University of Technology

Gaofeng Ren

Wuhan University of Technology

Zhen Wang

China University of Mining and Technology

Pulin Kang

Wuhan University of Technology

Article

Keywords: Radially decoupled explosive charge, Interval charging device, Fines proportion, Fragment size distribution

Posted Date: June 29th, 2026

DOI: https://doi.org/10.21203/rs.3.rs-9978977/v1

License: This work is licensed under a Creative Commons Attribution 4.0 International License.
Read Full License

Additional Declarations: Competing interest reported. The authors declare that they have no known competing financial interests or personal relationships that could have appeared to influence the work reported in this paper.

Version of Record: A version of this preprint was published at Scientific Reports on October 13th, 2026. See the published version at https://doi.org/10.1038/s41598-026-70032-4.

Abstract

To investigate the influence mechanism of a radial uncoupled charge structure using mixed emulsion explosives on the blasting fines generation rate, a typical granite mine was selected as the research case. a systematic study was conducted by integrating theoretical analysis, transparent tube simulations, and on-site industrial trials. First, by comparing coupled and uncoupled charges, we demonstrate the advantage of radially uncoupled charges in achieving peak detonation stress attenuation and uniform energy release through the annular gap. Second, variable-diameter radial decoupled spaced sinking charge simulations were conducted to optimize spacer installation and isolation measures. Finally, field trials were carried out on a weakly weathered (+ 30 m) and a moderately weathered (+ 45 m) granite bench within the same mine, where different decoupling coefficient schemes were applied to the upper, middle, and lower sections of bench-zoned areas and compared with traditional rock-slag spacers and continuous charging. Results show that in weakly to moderately weathered granite, this radially uncoupled configuration-with a 125 mm bottom charge and 110 mm middle/upper spacers-reduces unit explosive consumption by over 16%, yields a uniform block size distribution, lowers fines generation, and produces a moderately loose muckpile favorable for subsequent excavation and loading. This proposed structure effectively controls the pulverization rate in granite blasting, offering a technical reference for similar granite quarries.

1. Introduction

Blasting is widely used in mining and tunnel excavation projects.With the advancement of technology and progress in techniques, the proportion of intelligent blasting technology in production has been increasing year by year. For traditional open-pit aggregate mines, rock fragmentation caused by blasting constitutes the initial stage of mining operations and plays a crucial role in producing deliverable, marketable products(An et al., 2017, Li et al., 2022).Due to production constraints and slope control requirements, certain blasting operations necessitate the use of non-coupled charging patterns (including radial non-coupled and axial non-coupled charging).The so-called decoupling coefficient refers to the ratio of the charge diameter to the borehole diameter. Therefore, it is necessary to investigate the rock fragmentation behavior during blasting under decoupled charges to further optimize the design of blasting parameters, thereby enhancing the excavation and fragmentation performance of rock in both controlled blasting and production blasting(Li et al., 2023).

For traditional fully coupled charge structures, the high-pressure, high-temperature, and high-velocity detonation waves and products generated by explosive detonation directly impact the borehole wall rock, applying an extremely high impact load within an extremely short time. This causes the borehole wall rock to undergo intense compression and fragmentation, forming a “crushing zone” that consumes a significant amount of energy. Consequently, the rock fragmentation effect is poor and fails to meet production requirements(Diehl et al., 2000). To address this situation, decoupled charging technology is employed, involving the insertion of a medium between the explosives and the borehole wall to reduce and buffer the blasting energy. During detonation, the coupling medium between the explosives and the

borehole wall is intensely compressed by the high pressure generated from the expansion of detonation products, causing the explosive shock wave/stress wave within the coupling medium to rapidly attenuate(Chen et al., 2020). Through these mechanisms, as the gap between the explosives and the borehole wall thickens, the number of excessively fragmented rock particles generated near the borehole decreases, accompanied by the rapid formation and large-scale development of short fractures. When a lower coupling coefficient is used for borehole charging, rock fragmentation is primarily controlled by the propagation and interconnection of long fractures, forming a radial fracture pattern((Pál et al., 2014, Wittel et al., 2004), The rock distribution is uneven, with a high proportion of large fragments. Under normal circumstances, radially uncoupled charge structures can effectively enhance the energy utilization efficiency of explosives within rock formations(Guo Y et al., 2024, Ma T et al., 2022, Ding X et al., 2023, Guo Y et al., 2024, Wang Y et al., 2020). This method not only suppresses the generation of fine particles but also enhances the utilization efficiency of blasting energy, facilitating the formation of an ideal particle size distribution. By rationally designing the decoupling coefficient, the synergistic effect between stress waves and gas expansion can be regulated, thereby optimizing fragmentation results. By controlling the decoupling coefficient, the transmission efficiency of detonation wave energy within rock can be effectively adjusted, enabling precise control over the degree of rock fragmentation post-blasting. This approach demonstrates particularly significant results in hard rock bodies such as granite. Additionally, uncoupled charge structures are also influenced by coupling media, with air and rock debris being common examples. When air serves as the coupling medium, the explosive gases no longer act directly on the borehole wall, resulting in inefficient energy release. Simultaneously, due to air's low wave impedance, the transmission efficiency of stresses generated by the explosion from the explosive to the air and from the air to the rock is reduced. Similarly, rock debris also slows the release of explosive energy. By leveraging these mechanisms, air decoupling can be employed to reduce extreme rock fragmentation, typically used to mitigate damage and vibration in retained rock(Liu et al., 2019, Singh et al., 2014, Tose, 2006).

Against this background, this study, using a specific granite mine as its engineering context, employs a combination of theoretical analysis, transparent tube simulation tests and on-site industrial trials to systematically investigate the influence of radially uncoupled charging patterns on the fragmentation rate of fine-grained ore using mixed emulsion explosives. Firstly, a comparative analysis was conducted on the mechanisms of action and energy transfer characteristics of coupled and decoupled charging schemes; secondly, through simulated underground excavation tests using variable-diameter radial decoupling partitions, the installation process and isolation measures for the partitions were optimised; finally, industrial comparative tests were carried out on weakly and moderately weathered granite plateaus. Based on the mechanical properties of graded and zoned sections, charging schemes with different decoupling coefficients were designed, and the variation patterns of the particle size distribution of blasted blocks and the rate of fine ore were investigated at different locations. The research findings provide a theoretical basis and technical support for efficient, low-consumption blasting operations in granite mines.

2. Materials and Methods

2.1 Experimental Materials

The main equipment used in this test includes site-mixed emulsion explosives, primer charges, detonating cord, and a self-developed variable-diameter radial uncoupled spacer.

The on-site test used prefabricated strip-type emulsion explosives(Figs. 1). The density of these explosives ranged from 1.10 to 1.25 grams per cubic centimeter, the detonation speed was 4500 to 5000 meters per second, and the detonation heat was approximately 3500 kilojoules per kilogram. Detonation was achieved using detonating cords, with a delay time of 25 milliseconds inside the hole, and 45 milliseconds and 65 milliseconds between rows.

The radial uncoupled spacer used in this study was a self-developed variable-diameter structure, mainly composed of three parts (Figs. 2):

Tube body: the main part forming the charge cavity, available in different diameters (Φ125 mm, Φ110 mm, Φ90 mm) as required;

Explosive receiver: a funnel-shaped structure with a wide upper opening and a narrow lower end, with its upper outer edge designed to fit tightly against the borehole wall and its lower part connected to the connector, responsible for guiding the explosive into the tube body;

Connector: used to connect various components and ensure structural sealing.

By combining tube sections with different diameters, this spacer enables the formation of an axially continuous, radially uncoupled charge structure within the borehole, achieving differential distribution of explosive energy along the hole depth.

2.2 Simulation experiment

To simulate the working condition of the radial uncoupled spacer in an actual blast hole, a transparent tube simulation system was designed and constructed. The main apparatus was a 4.0 m long anti-static transparent polycarbonate tube with an inner diameter of 140 mm, vertically fixed to simulate a vertical blast hole. This inner diameter is consistent with the actual field blast hole diameter (140 mm) to ensure geometric similarity. A 20 cm thick layer of crushed rock slag was pre-filled at the bottom of the tube to simulate the actual residual debris environment at the borehole bottom.

To systematically evaluate the installation process, sealing performance, and sinking behavior of the spacer in the explosive, three sets of simulation tests were designed, each repeated three times to ensure data reliability.

Test I: Free-fall embedding test of spacer

The spacer was released vertically into the center of the transparent tube with an initial acceleration, allowing it to fall freely to the tube bottom. The embedding depth into the rock slag layer and the stability of the spacer were observed.

Test II: Explosive charging and backfill mixing test

The delivery hose of the on-site mixing and charging truck was aligned vertically with the tube opening, and emulsion explosive was pumped into the tube at the actual field charging pressure to a depth of 2.0 m. After standing for 15 min, rock slag was backfilled into the tube to the designed height. The degree of mixing between explosive and slag at the bottom and at the charge height was observed.

Test III: Sinking behavior of spacer in explosive and secondary charging test

First, 2.0 m depth of emulsion explosive was charged into the transparent tube, and then the spacer was placed into the tube. The sinking rate and depth of the spacer were observed. After the spacer stabilized, additional emulsion explosive was charged into the spacer, and any secondary sinking and its rate were recorded.

2.3 Field Industrial Tests and Blasting Parameters

Field comparative tests were conducted on the + 30 m platform (weakly weathered granite) and the + 45 m platform (moderately weathered granite). For each platform, two blasting areas with similar geological conditions were selected as the test section and the control section (Figs. 3). The test section employed the newly developed spacer to achieve radial uncoupled axial continuous charging, while the control section used the traditional rock slag interval charging method.

The blasting parameters were as follows:

Bench height: 15 m

Sub-drilling: 1.5 m

Borehole diameter: 140 mm

Burden: 4.0 m (weakly weathered), 4.2 m (moderately weathered)

Spacing: 6.5 m (weakly weathered), 7.0 m (moderately weathered)

Bottom resistance line: 4.0 m (weakly weathered), 4.2 m (moderately weathered)

Initiation network: in-hole delay of 25 ms, inter-row delays of 45 ms and 65 ms.

The specific charging schemes are presented in Table 1. The control group adopted rock slag interval charging, with a charge height of 9.5 m, stemming length of 7 m, and a single-hole charge weight of 190 kg. Test Group I employed a radial uncoupled structure with a Φ125 mm charge section at the bottom (4

m) and a Φ110 mm charge section at the upper part (9 m). Test Group II employed a three-stage radial uncoupled structure with a Φ125 mm bottom section (4 m), a Φ110 mm middle section (4 m), and a Φ90 mm upper section (5 m).

Table 1
On-site blasting test parameters table

Degree of rock weathering		Loading height (m)	Blocked section (m)	Single-well dosage (kg)	Design unit consumption (kg/m³)	Loading method
Weak weathering	Control	9.5	7	190	0.49	Rock slag is loaded at intervals
	I	13	3.5	160	0.41	The spacer is used, with the bottom 4m (F125mm) and the top 9m (F110mm).
	□	13	3.5	139	0.36	Using spacers, the bottom is 4m (Φ125mm), the middle is 4m (Φ110mm), and the top is 5m (Φ90mm)
Moderate weathering	Control	9.5	7	190	0.43	Rock slag is loaded at intervals
	I	13	3.5	160	0.36	The spacer is used, with the bottom 4m (Φ125mm) and the top 9m (Φ110mm).
	□	13	3.5	139	0.32	Using spacers, the bottom is 4m (Φ125mm), the middle is 4m (Φ110mm), and the top is 5m (Φ90mm)

2.4 Data Collection and Analysis Methods

After blasting, on-site observations were conducted on the muck pile, focusing on the following indicators:

Fragmentation distribution: determined by a combination of image analysis and sieve testing to calculate the proportion of each particle size range;

Fines ratio: defined as rock particles with a particle size < 5 mm, calculated by weighing the mass proportion of fines;

Boulder ratio: defined as rock blocks with a particle size > 1000 mm, counting their quantity and distribution;

Muck pile morphology: including the looseness of the muck pile, the smoothness of the slope surface, and the presence of residual toes or overhangs.

3. Results

3.1 Simulation Test Results

Field test phenomena of the spacer device are as follows(Fig. 4):

Spacer Embedding Depth: In Test I, under free-fall impact, the spacer embedded into the bottom rock slag layer to a depth of 2–3 cm. The spacer achieved initial anchoring in the bottom slag by its own weight, demonstrating preliminary stability but limited embedding depth.

Explosive-Slag Mixing Characteristics: In Test II, no emulsion explosive seepage was observed from the bottom of the transparent tube. However, a 5–7 cm thick layer of explosive at the bottom mixed with the rock slag, rendering this portion ineffective. After standing for 15 min with backfilled slag, the mixed zone expanded to 10–15 cm, further increasing explosive failure .

Spacer Sinking Behavior: In Test III, under different initial acceleration conditions, the spacer inserted into the explosive to a depth of 1.2–1.7 m after 15 min, with the remaining portion suspended above the explosive. After additional explosive was charged into the spacer, continued sinking occurred but eventually stabilized.

3.2 Field Industrial Test Results

The results of the test blasts for each group under the two schemes are shown in Fig. 5. The control group employed either intermittent or continuous charging of rock waste, achieving a high fine ore rate post-blast with virtually no large rock fragments. This indicates that traditional methods are effective in suppressing the generation of large rock fragments. However, due to concentrated energy, the issue of rock over-crushing remains prominent.

For Scheme 1, Test Group I employed spacers for weakly weathered granite, setting the diameter of the upper-middle uncoupled section to 110 mm with an uncoupling coefficient of 1.27. This reduced the unit explosive consumption by 16.3% compared to the control group. Post-blast, rock block size distribution exhibited uniformity with no significant accumulation of large boulders or fine rock. The blast pile showed good looseness, enabling high excavation and loading efficiency. Test Group II set the middle decoupled section diameter at 110 mm and the upper section at 90 mm, with an upper decoupling

coefficient of 1.55, achieving a 26.5% reduction in unit explosive consumption compared to the control group. Post-blast analysis revealed a significant increase in surface large-block rates. The upper section's explosive energy proved insufficient for adequate rock fragmentation, resulting in poor blast pile looseness and reduced excavation and loading efficiency. Additionally, localized “umbrella rock” phenomena occurred along the crest line.

Test Group I used spacers in moderately weathered granite for Scheme 2, with a decoupling coefficient of 1.27 and an upper-middle decoupled section diameter of 110 mm. In comparison to the control group, this led to a 16.2% decrease in the amount of explosives consumed per unit. Following the blast, there was no discernible buildup of big boulders or fine ore, and the distribution of rock block sizes was homogeneous. High excavation and loading efficiency was made possible by the blast pile's good looseness. By lowering the upper decoupled section diameter to 90mm and setting the decoupling coefficient to 1.56, Test Group II further optimized the decoupling structure, resulting in a 25.6% decrease in explosives consumption per unit volume when compared to the control group. A post-blast examination showed that the proportion of huge rock on the blast pile surface had moderately increased, the percentage of fine ore had further decreased, and the loose rock condition was suitable. There was no discernible formation of a rock bed. Excavation and loading efficiency were not negatively impacted by secondary crushing using a rock breaker.

3.3 Dimensions and Distribution

In order to further quantify the blasting effects under different rock types and different charge structures, the Split Engineering Split-Desktop software was used to analyze the morphological characteristics of the blasting pile. The processed blasting pile is shown in Fig. 6. Meanwhile, the particle size distribution curves of each charge structure and weathering types were plotted, as shown in Fig. 7.

In the weakly weathered granite, the size distribution of the control group (rock debris spaced for detonation) exhibited a "central concentration and lower values at both ends" characteristic of a normal distribution. The fragmentation uniformity was good, with a cumulative percentage of the 0–1 cm size range reaching 6.84%, while the proportion of large blocks (> 100 cm) was 0.67%, and the medium-sized size range (10–15 cm) had the highest proportion, reaching 24.05%. This indicated that although the traditional detonation structure could effectively control the generation of large blocks, the energy was too concentrated, resulting in smaller block sizes in the fragmentation area and a higher proportion of fine particles, which would easily lead to a decrease in the efficiency of subsequent screening and transportation. In test group I, a radial un-coupled detonation structure with a bottom of 125 mm and upper middle part of 110 mm was adopted. The cumulative percentage of the 0–1 cm size range decreased to 3.41%, and the distribution of the medium-sized size range (15–50 cm) became more uniform, with a proportion of 64.7%. This significantly improved the blasting pile grading structure, making the fragmentation products more in line with the requirements of subsequent crushing and screening processes. It was shown that the moderately un-coupled detonation structure effectively reduced the proportion of small particles while ensuring the full development of the main fracture zone. Test group II adopted a three-stage un-coupled structure (bottom 125 mm, middle 110 mm, upper 90

mm). Compared with the control group, the percentage of large blocks after blasting increased to 3.91%, and the large blocks were mainly concentrated on the surface of the blasting pile and the top of the platform, which was closely related to the excessive un-coupling coefficient (1.55) in the upper part, resulting in insufficient energy. It was concluded that this was due to insufficient energy in the upper part of the fragmentation, causing some areas of the rock mass not to be fully fractured.

In the weathered granite, the proportion of fine powder minerals in the control group reached as high as 8.93% (particle size < 1 cm), which was much higher than that of the other two experimental groups, showing a distinct "fine particle concentration" feature. This was due to the development of joint fissures in the weathered granite. Under continuous loading conditions, the explosion energy was rapidly released along the original fissures, intensifying the over-crushing of the rock mass. In the test group I, the content of fine powder minerals was reduced to 5.63%, and the distribution of each particle size range became more uniform. The proportion of medium-sized particles (15–50 cm) increased to 48.34%, and the rate of large blocks was controlled at 1.81%. This indicates that the radial uncoupling structure attenuated the initial impact pressure through air gaps, effectively inhibiting the excessive release of energy along the fissures, and achieving a transformation from "over-crushing along the fissures" to "uniform overall fragmentation". In test group II, the proportion of fine powder minerals was further reduced to 4.59%, but the rate of large blocks increased significantly to 4.67%. Unlike weakly weathered granite, this group did not show obvious "umbrella rock" phenomenon after blasting. The loose degree of the blasting pile was good, and it did not have a negative impact on the loading efficiency, reflecting that the weathered granite has stronger adaptability to insufficient upper energy: its developed original fissures can assist in fragmentation under the "wedge effect" of the explosion gas, to some extent, compensating for the lack of impact energy.

By comparing the size distribution characteristics of the two rock types, the rock type compatibility boundary for optimization of the uncoupling coefficient can be revealed. The weakly weathered granite has high hardness and poorly developed fractures, and is highly sensitive to the initial impact energy. When the upper uncoupling coefficient reaches 1.55, the impact energy decays excessively, making it difficult to form an effective initial fracture network, resulting in a significant increase in the rate of large blocks (3.91%). This type of rock mass has a lower "tolerance" to the uncoupling coefficient and the uncoupling coefficient should be controlled within 1.12 to 1.27 to ensure sufficient impact energy for crack initiation. The moderately weathered granite has developed primary fractures and the fragmentation mechanism combines both "impact fragmentation" and "gas wedge entry" effects. Even when the upper uncoupling coefficient is raised to 1.55, the explosion gas can still expand along the primary fractures to form auxiliary fragmentation, so the increase in the rate of large blocks is limited (from 0.17% to 4.67%), and no obvious fragmentation blind zone occurs. It has a stronger adaptability to the uncoupling coefficient and greater potential for energy conservation. From the perspective of energy matching, the test group I achieved a gradient energy distribution of "moderate enhancement at the bottom and moderate weakening in the middle and upper parts" in both rock types, which formed a good match with the stepwise zone load-bearing characteristics (high constraint at the bottom and low constraint at the top). Test group II showed an energy "supply-demand imbalance" in the weakly

weathered rock, confirming the existence of an engineering applicable boundary for "excessive uncoupling coefficient".

The above analysis indicates that the optimization of the radial uncoupled explosive loading structure needs to comprehensively consider the mechanical properties of the rock, the force distribution characteristics of the step divisions, and the engineering requirements. In the test group Ⅸ, a gradient energy distribution of "moderate enhancement at the bottom and moderate weakening in the middle and upper parts" was achieved in both rock types, which is in good match with the force distribution characteristics of the step divisions (high constraint at the bottom and low constraint at the top), and is the optimal explosive loading scheme.

4. Discussion

Through on-site industrial experiments, this study found that using a radial uncoupled charge structure with a "bottom diameter of 125 mm and middle-upper part diameter of 110 mm" can significantly reduce the specific explosive consumption (by more than 16%) in both weakly weathered and moderately weathered granite. At the same time, it achieves a uniform fragment size and a controllable fine ore percentage, resulting in a favorable overall blasting effect. This finding is consistent with previous studies (Liu et al., 2024; Huo et al., 2023), which demonstrated that uncoupled charges can reduce the blast hole radius and suppress the generation of fines. However, this study further reveals the zoning adaptability advantage of the radial uncoupled structure in bench blasting.

Regarding the energy transfer mechanism, the radial uncoupled charge effectively attenuates the initial peak pressure of the detonation wave through the annular air gap, transforming the impact load on the borehole wall from "instantaneous high intensity" to "continuous and stable," thereby avoiding excessive pulverization of the near-field rock mass (Kakogiannis et al., 2010). Simultaneously, the air gap provides expansion space for explosive gases, prolongs the duration of quasi-static pressure, and promotes stable crack growth and coalescence (Cho et al., 2004). This energy distribution strategy of "peak reduction and gas extension" is the core mechanism for achieving control over the fine ore percentage.

It is worth noting that in Test Group II (with an upper uncoupling coefficient of 1.55), although the specific explosive consumption was further reduced (by 25.6%), an increase in the boulder rate and the occurrence of "umbrella rock" were observed in weakly weathered granite. In contrast, the effect was more ideal in moderately weathered granite. This discrepancy indicates that there is a rock-type adaptation boundary when optimizing the uncoupling coefficient. Weakly weathered granite, being harder and less jointed, is more sensitive to initial impact energy; an excessively large uncoupling coefficient leads to insufficient energy and ineffective crack initiation. Moderately weathered granite, however, contains pre-existing fractures that can utilize the "gas wedge effect" of explosion gases along these fractures to achieve fragmentation, making it less dependent on initial impact energy.

Furthermore, the differences in stress distribution across different parts of the bench during blasting are key factors influencing the distribution of fines and boulders. Theoretical analysis clarifies that the bench

bottom, characterized by high confining pressure and strong constraints, is prone to stress concentration and fine generation, whereas the upper part, with more free surfaces and weaker constraints, tends to produce boulders due to insufficient energy. This "strong bottom, weak top" stress gradient inherently requires a charge structure capable of achieving differentiated axial energy distribution. Traditional uniform or simple segmented charges cannot meet this requirement. In this study, an axial variable-radius uncoupled charge structure was adopted: using a smaller uncoupling coefficient (1.12, Φ125 mm) at the bottom via a spacer, and a larger uncoupling coefficient (1.27, Φ110 mm) in the middle and upper parts. This configuration achieves a gradient energy distribution characterized by "moderate enhancement at the bottom and moderate weakening at the top." Consequently, the explosive energy and rock resistance form an opposing match along the axial direction: the bottom region receives sufficient energy to overcome high confining pressure and ensure toe removal, while the upper region avoids excessive energy, reducing the fines rate.

The on-site test results validate the above mechanism. Both Test Group I of Scheme One and Test Group I of Scheme Two achieved uniform fragment sizes and controllable fines. In contrast, Test Group II of Scheme One, with an excessively high upper coupling coefficient (1.55), suffered from severe energy deficiency in the upper part and a marked increase in the boulder rate. This provides counterevidence to the theoretical judgment that "insufficient upper energy is the main cause of boulder generation."

In terms of charge structure comparison, this study systematically observed the working state of the radial uncoupled spacer using transparent tube simulation tests and compared it with traditional rock-debris spaced charging. The results show that traditional rock-debris spaced charging suffers from explosive mixing (10–15 cm), leading to charge failure, imprecise control of spacer position, and random energy distribution. In contrast, the radial uncoupled spacer achieves precise positioning and sealed isolation of charge segments through a mechanical structure, creating a controllable radial uncoupling effect. Previous research (Liu et al., 2024) analyzed the spatiotemporal evolution characteristics of the explosion strain field and crack field in a radial uncoupled medium, as well as the energy distribution mechanism, using theoretical derivations combined with dynamic caustics and DIC experimental systems. The present study further confirms this viewpoint through industrial experiments: the radial uncoupled structure can precisely control the uncoupling coefficient by adjusting the explosive diameter ratio, achieving "on-demand allocation" of explosion energy, whereas axial spaced charging can only alter the distribution range of energy within the borehole and struggles to regulate the peak value or mode of energy release. Therefore, for hard-rock bench blasting requiring precise control of the fine ore percentage, the radial uncoupled structure offers an irreplaceable advantage.

In summary, through the "peak reduction and gas extension" energy distribution mechanism and the axial gradient energy distribution design, the radial uncoupled charge structure effectively accommodates the "strong bottom, weak top" stress gradient characteristic of bench blasting, achieving coordinated control of both fine ore percentage and boulder rate. Meanwhile, optimization of the uncoupling coefficient should fully consider lithological differences to achieve the best performance.

5. Conclusion

This study systematically investigated the influence of radial decoupled charging structures for mixed-charge emulsion explosives on the pulverization rate of granite ore. Through theoretical analysis, transparent tube simulations, and field industrial trials, it identified optimal charging parameters and technical solutions for rock layers with varying degrees of weathering. Key findings include:

(1) A comparative analysis was conducted on the principles and performance metrics of coupled and uncoupled charge structures, while also examining the advantages of radially uncoupled charges over axially spaced charges. By integrating the stress characteristics of different sections in bench blasting, the primary zones contributing to high lump rates and fine ore rates were identified, and targeted solutions were proposed.

(2) For granite with varying degrees of weathering, a radial decoupled charging structure was employed under established borehole network parameters: a 125mm diameter charge (decoupling coefficient 1.12) at the bottom of the borehole and a 110mm diameter charge (decoupling coefficient 1.27) in the middle and upper sections. This approach achieved controllability in the on-site mixed emulsion explosive charging structure. Based on this approach, the comprehensive unit consumption of explosives decreased by approximately 15%. Post-blast, the block size distribution of the blast pile exhibited uniformity, with loose material maintained at an optimal level, while simultaneously achieving the objective of reducing the powder ore rate.

(3) The optimization of the decoupling coefficient has a lithology adaptation boundary. Weakly weathered granite has high hardness and poorly developed joints, making it more sensitive to the initial impact energy. An excessively large decoupling coefficient (such as 1.55) will result in insufficient energy at the upper part and an increase in the proportion of large fragments; while moderately weathered granite, due to the development of primary fractures, can achieve fragmentation through the "gas wedge effect" along the fractures, and has relatively lower dependence on the initial impact energy. Under the same decoupling coefficient, it can achieve a better fragmentation effect.

Declarations

Funding

This work was supported by the National Natural Science Foundation of China (Grant Nos. 52174087).

Declaration of Conflict of interest

The authors declare that they have no known competing financial interests or personal relationships that could have appeared to influence the work reported in this paper.

Author Contribution Statement

Tao Wang: Conceptualization, Investigation, Methodology, Validation, Writing – original draft, Visualization, Software.

Gao-feng Ren: Conceptualization, Resources, Supervision, Project administration, Funding acquisition, Writing – review & editing.

Zhen Wang: Data curation, Formal analysis, Investigation, Validation, Writing-review & editing.

Pu-lin Kang: Investigation, Data curation, Visualization, Software, Writing.

All authors have read and agreed to the published version of the manuscript.

Data Availability Statement

The data that support the findings of this study are available from the corresponding author upon reasonable request.

References

1. An, H. M., Liu, H. Y., Han, H., Zheng, X., & Wang, X. G. (2017). Hybrid finite-discrete element modelling of dynamic fracture and resultant fragment casting and muck-piling by rock blast. *Computers and Geotechnics*, 81, 322-345. DOI:10.1016/j. compgeo.2016.09.007.
2. Li, X., Liu, K., Yang, J., & Song, R. (2022). Numerical study on blast-induced fragmentation in deep rock mass. *International Journal of Impact Engineering*, 170, 104367. DOI:*10.1016/j.ijimpeng.2022.104367*.
3. Li, X., Liu, K., Sha, Y., Yang, J., & Song, R. (2023). Numerical investigation on rock fragmentation under decoupled charge blasting. Computers and Geotechnics, 157, 105312.DOI:*10.1016/j.compgeo.2023.105312*.
4. Diehl A, Carmona H A, Araripe L E, et al. (2000) Scaling behavior in explosive fragmentation. Physical Review E, 62(4), 4742. DOI:*10.1103/PhysRevE.62.4742*.
5. Chen M, Ye Z, Lu W, et al. (2020). An improved method for calculating the peak explosion pressure on the borehole wall in decoupling charge blasting. International Journal of Impact Engineering, 146,103695. DOI:*10.1016/j.ijimpeng.2020.103695*.
6. Pál G, Varga I, Kun F. (2014). Emergence of energy dependence in the fragmentation of heterogeneous materials. Physical Review E, 90(6), 062811. DOI:*10.1103/PhysRevE.90.062811*.
7. Wittel F, Kun F, Herrmann H J, et al. (2004). Fragmentation of shells. Physical Review Letters, 93(3), 035504. DOI:*10.1103/PhysRevLett.93.035504*.
8. Guo Y, Yang R, Peng S. et al. (2024). Experimental study on decoupled charge blasting-induced crack propagation with parabolic shaped charge. Engineering Fracture Mechanics, 304,110178. DOI:10.1016/j.engfracmech.2024.110178.

9. Ma T, Li F, Yang Y, et al. (2022). Study on energy evolution and crack propagation of rock mass under single hole uncoupled charge blasting. Applications in Engineering Science, 11,100112. DOI:10.1016/j.apples.2022.100112.
10. Ding X, Liu X, Ao Z, et al. (2023). Research on blasting mechanism and blasting effect of aqueous media in open pit coal mines. *Scientific Reports*, 13(1),19140. DOI:10.1038/s41598-023-46449-6.
11. Guo Y, Yang R, Peng S, et al. (2024). Experimental study on decoupled charge blasting-induced crack propagation with parabolic shaped charge. *Engineering Fracture Mechanics*, 304,110178. DOI:10.1016/j.engfracmech.2024.110178.
12. Wang Y, Wen Z, Liu G, et al. (2020). Explosion propagation and characteristics of rock damage in decoupled charge blasting based on computed tomography scanning. *International Journal of Rock Mechanics and Mining Sciences*, 136,104540. DOI:10.1016/j.ijrmms.2020.104540.
13. Liu K, Li X, Hao H, et al. (2019). Study on the raising technique using one blast based on the combination of long-hole presplitting and vertical crater retreat multiple-deck shots. *International Journal of Rock Mechanics and Mining Sciences*, 113,41-58. DOI:10.1016/j.ijrmms.2018.11.012.
14. Singh P K, Roy M P, Paswan R K. (2014). Controlled blasting for long term stability of pit-walls. *International Journal of Rock Mechanics and Mining Sciences*, 70,388-399. DOI:10.1016/j.ijrmms.2014.05.006.
15. Tose S S J. (2006). A review of the design criteria and practical aspects of developing a successful pre-split. Stability of Rock Slopes in Open Pit Mining and Civil Engineering Situations, 525-546.
16. Liu, K., Li, X., Yang, J., Zhou, Z., Sha, Y., & Hong, Z. (2024). Experimental and numerical investigation on rock fracturing and fragmentation under coupled static pressure and blasting. *Engineering Fracture Mechanics*, 311, 110593. DOI:10.1016/j.engfracmech.2024.110593.
17. Huo, X., Qiu, X., Shi, X., Chen, H., Zong, C., & Xie, C. (2023). Attenuation characteristics of blasting stress under decoupled cylindrical charge. Rock Mechanics and Rock Engineering, 56(6), 4185-4209. DOI:10.1007/s00603-023-03286-3.
18. Kakogiannis, D., Van Hemelrijck, D., Wastiels, J., Palanivelu, S., Van Paepegem, W., Vantomme, J., & Kostopoulos, V. (2010). Assessment of pressure waves generated by explosive loading. Computer Modeling in Engineering and Sciences (CMES), 65(1), 75. DOI:10.3970/cmes.2010.065.075.
19. Cho, S. H., Nakamura, Y., & Kaneko, K. (2004). Dynamic fracture process analysis of rock subjected to stress wave and gas pressurization. International Journal of Rock Mechanics and Mining Sciences, 41(SUPPL. 1), 2A-20. DOI:10.1016/j.ijrmms.2003.12.081.
20. Liu, Z., Yang, R., Zhao, Y., Zuo, J., Ding, C., Li, Y., & He, S. (2026). The Multi-field Evolution Mechanism of Radial Decoupled Medium Explosive Characteristics: Z. Rock Mechanics and Rock Engineering, 1-24. DOI:10.1007/s00603-026-05281-w.

Figures



Figure 1

Emulsified explosives and detonating cord

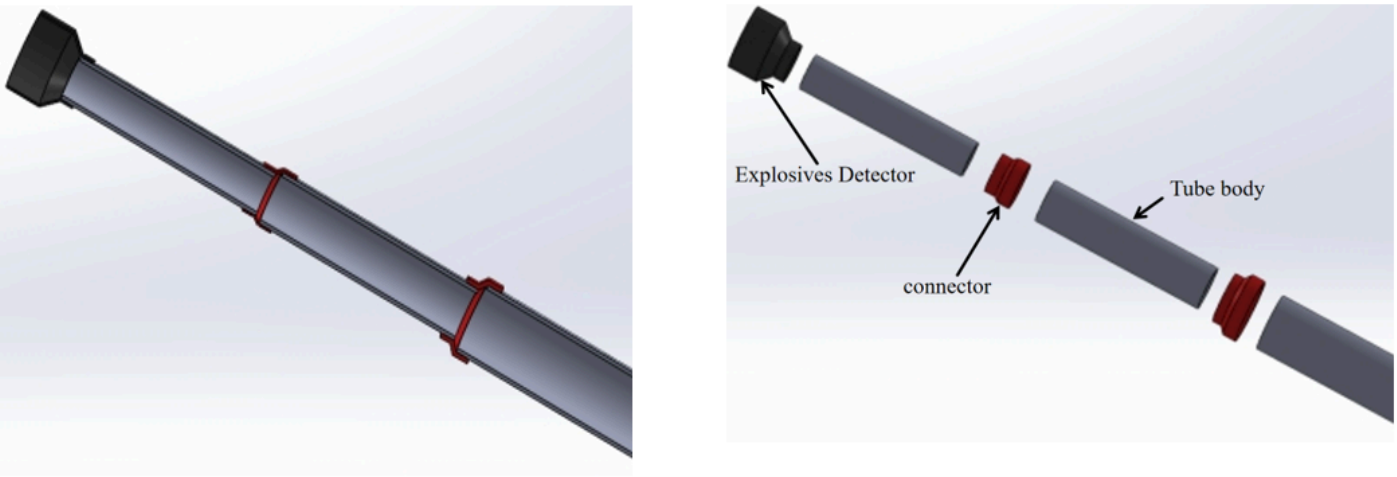


Figure 2

Schematic diagram of the interval device structure

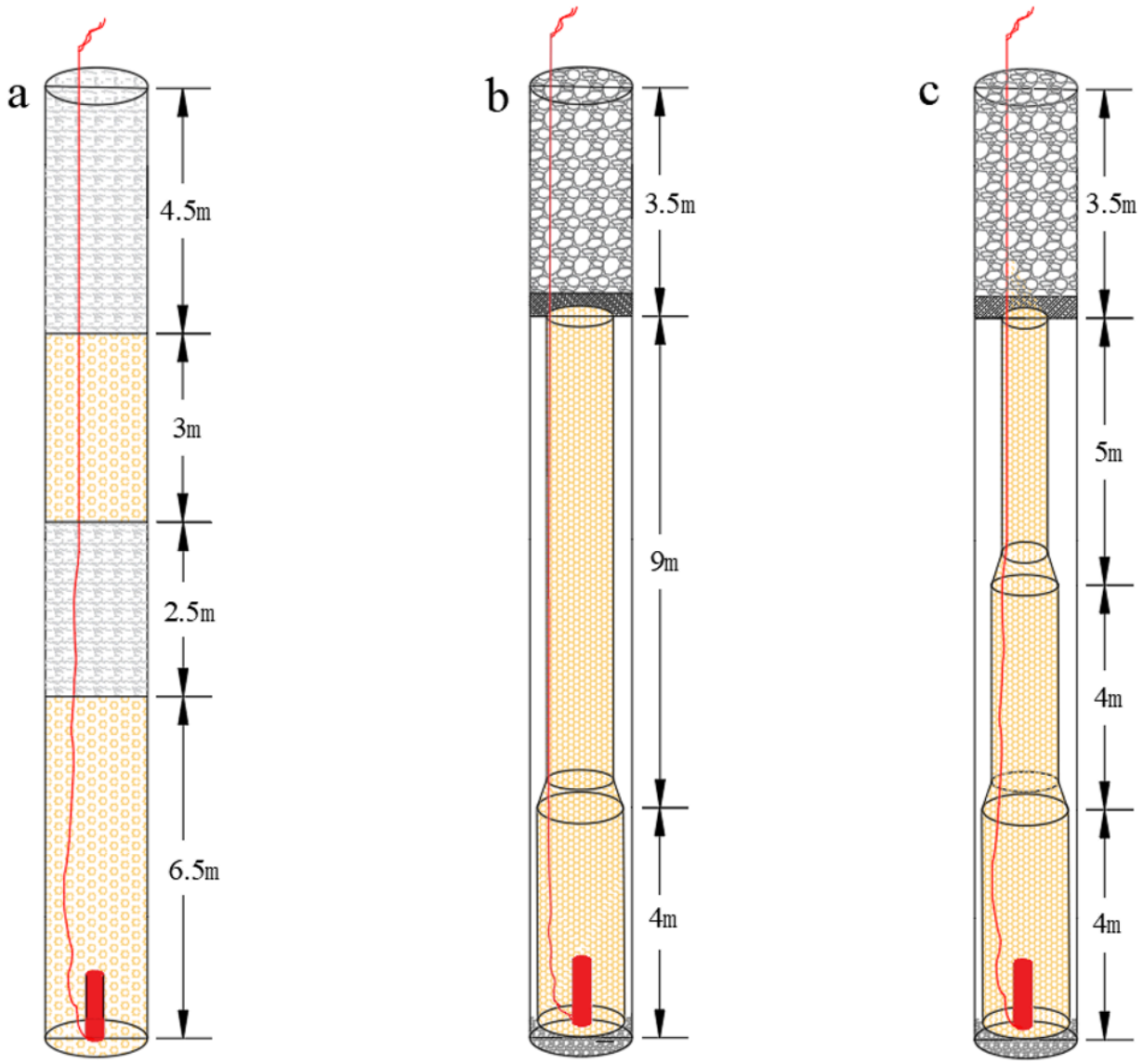


Figure 3

Industrial test charge loading structure diagram:(a) Rock slag is loaded at intervals;(b) Experiment Ⅰ Assembled Drug structure;(c) Experiment II Assembled Drug Structure



Figure 4

Field test of the spacer sinking:(a) Gun hole simulation; (b)Backfill rock debris at the bottom of the hole; (c)Backfill with rock slag;(d) Spacer settlement measurement

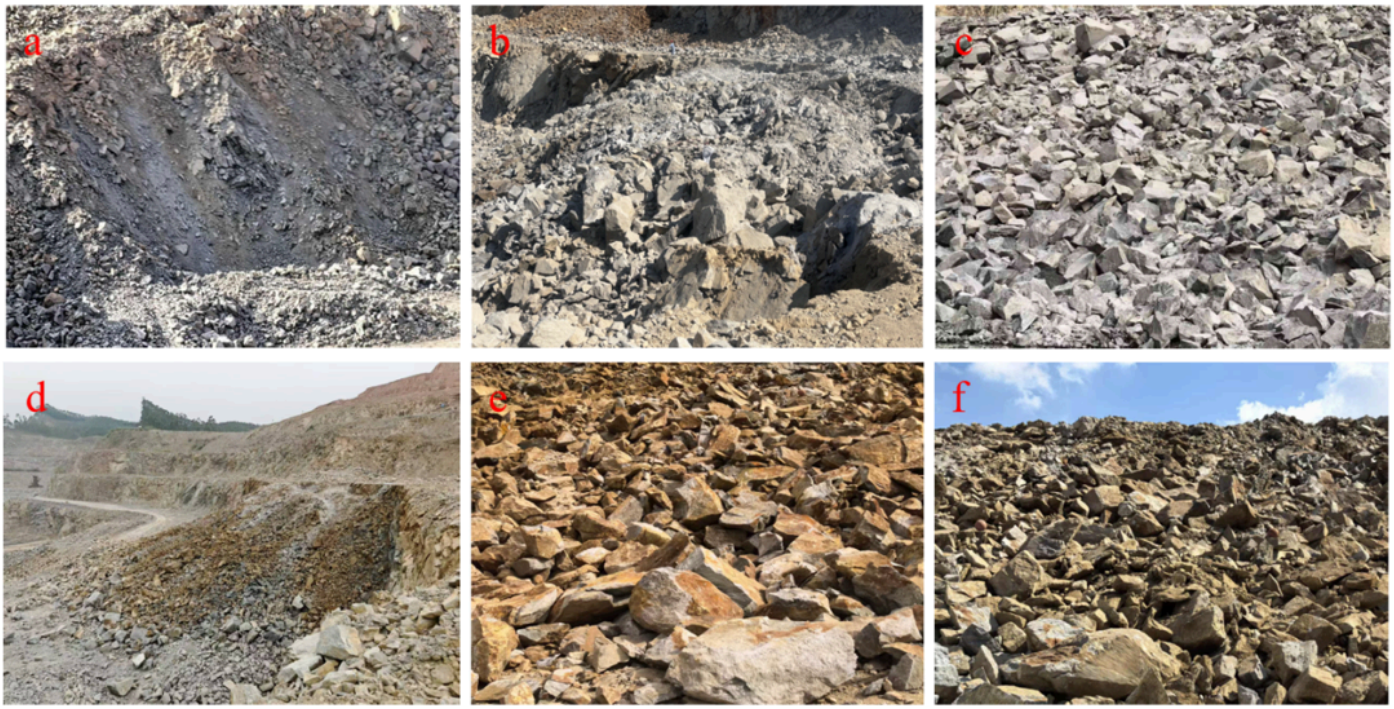


Figure 5

effect diagrams of each scheme after the explosion:(a)The weakly weathered control group;(b)Weakly weathered experimental group I;(c)Weakly weathered experimental group II;(d)Stroke control group; (e)Stroke-like experimental group I; (f)Stroke-like experimental group II

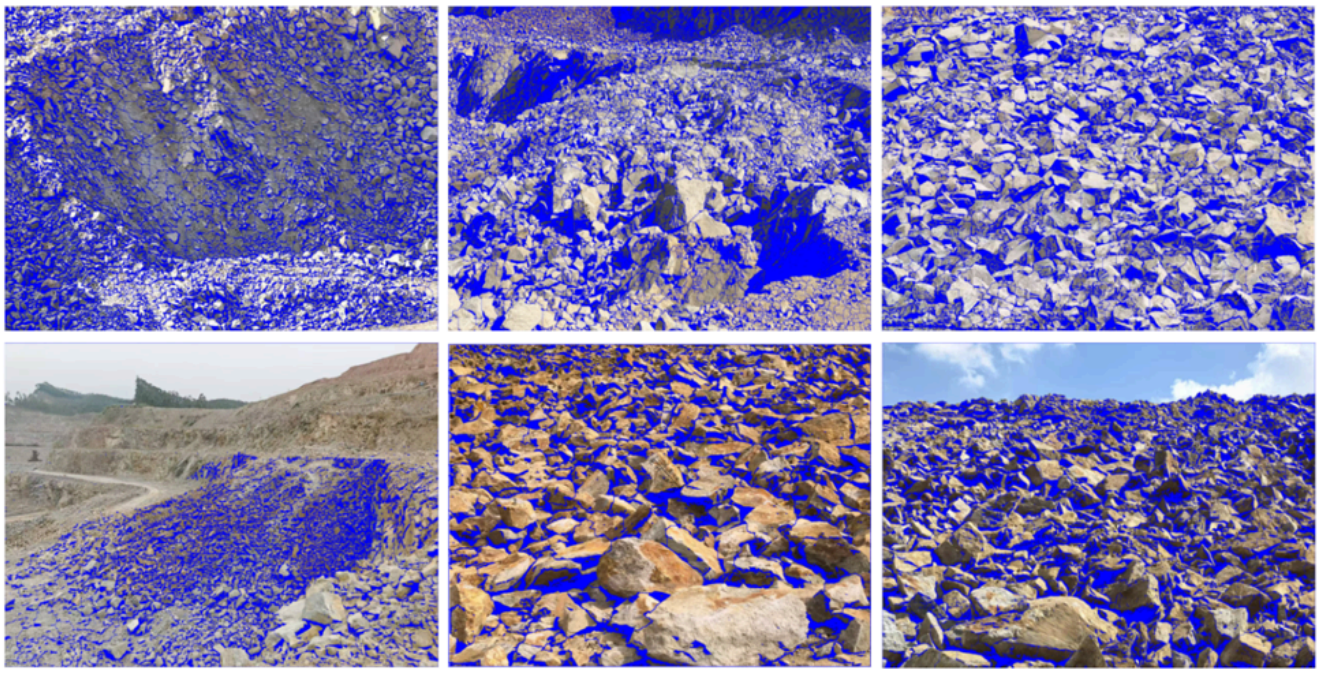


Figure 6

Heap formation characteristics

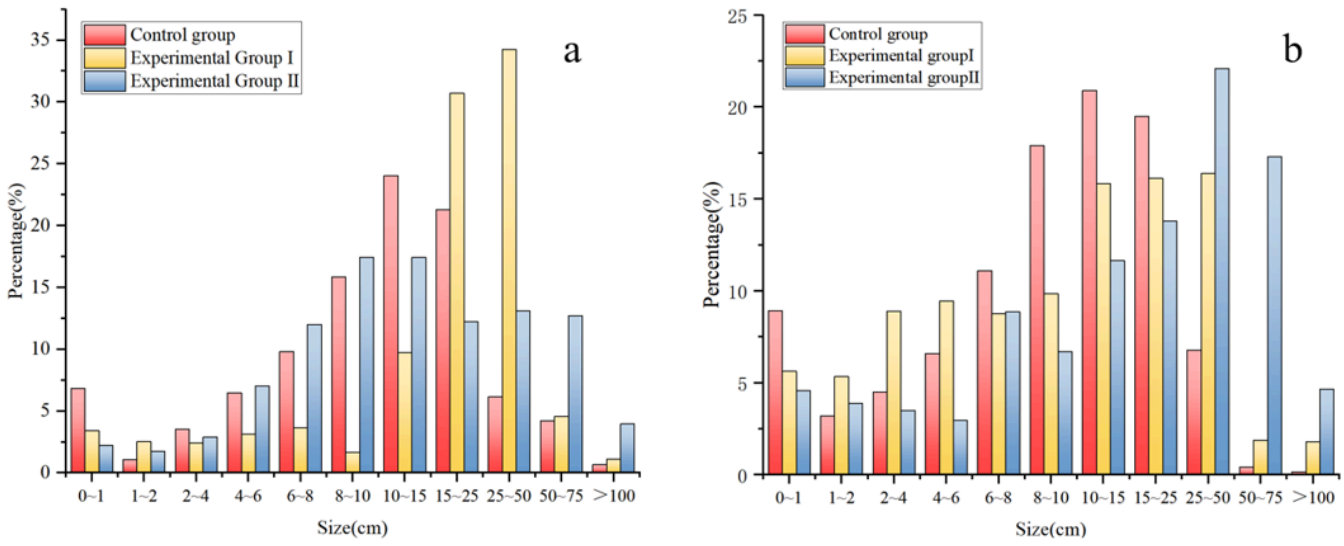


Figure 7

Particle size distribution curve: (a) Slightly weathered granite;(b) Sandy metamorphic granite